Ninth International Conference on
THIN-WALLED STRUCTURES – ICTWS2023
Sydney, Australia, Nov 29 – Dec 1, 2023

LOCAL BUCKLING DESIGN FOR HYBRID STEEL I-GIRDERS

Shuxian Chen *, Jun-zhi Liu ** and Tak-Ming Chan *

* Department of Civil and Environmental Engineering, The Hong Kong Polytechnic University, Hong Kong, China
e-mails: shuxian33.chen@polyu.edu.hk, tak-ming.chan@polyu.edu.hk

** School of National Safety and Emergency Management, Beijing Normal University, Zhuhai, China
e-mail: jun-zhi.liu@bnu.edu.cn

Keywords: High strength steel; Local buckling; Hybrid design; I-girder.

Abstract. *For I-sections subject to bending, the flange plates contribute more to the bending resistance than the web. In recent years, hybrid I-girders with higher strength flanges than the web have garnered increased interest due to their potential for optimal material utilisation. This article summarises available experimental studies in the literature, as well as current design rules in European codes and American specifications for the design of steel bridges, on the local buckling behaviour of hybrid I-girders. To expand the data pool, an experimental study of hybrid I-girders was conducted in this study using moment gradient and uniform bending tests. Two types of hybrid I-sections were investigated: (1) with Q690 flanges and Q460 web; and (2) with Q690 flanges and Q355 web, along with their homogeneous Q690 counterparts. The web slenderness was designed to cover Class 1 to Class 4 in accordance with Eurocode 3. Experimental observations of test specimens were discussed, and the specified design provisions in codes were compared with test results.*

1 INTRODUCTION

Owing to high strength-to-weight ratio, high strength steel (HSS) characterised with the nominal yield strength $f_{y,nom}$ not less than 460 MPa, has gained increased popularity in recent years. Hybrid design utilises varying strength grades for the constituent plates of steel sections, allowing for optimal material usage under various loads. I-sections under flexure commonly use higher strength steel for the flange plates, because of their greater contribution to the bending resistance than the web.

Studies on the local buckling behaviour of hybrid I-section flexural members date back to the 1960s. Table 1 summarises hybrid I-section bending tests reported in literature. In this table, "4PB" and "3PB" mean four-point and three-point bending tests, respectively; f_{yw}/f_{yf} denotes the web-to-flange yield strength ratio; the web slenderness λ_w is expressed by Equation (1), where h_w and t_w are the height and thickness of the web plate, and E represents the material's elastic modulus.

$$\lambda_w = \frac{h_w}{t_w}\sqrt{\frac{f_{yf}}{E}} \tag{1}$$

The earliest reported experiments on the local buckling behaviour of hybrid I-girders were conducted by researchers in the U.S. [1,2]. The test results showed that the yielding and buckling of the lower strength web have limited impact on the bending behaviour of hybrid I-girders. Based on these findings, the Joint AISC-AASHO Committee on Flexural Members [3] advised that the design of hybrid I-section flexural members may simply be based on the flange-

yield moment which causes the initiation of flange yielding, and the web yielding in hybrid sections can be disregarded. This statement lays the foundation of the hybrid design in American specifications since then. In Europe, Kamtekar et al. [4,5] experimentally studied the bending behaviour of hybrid I-girders, and the beneficial effect of strain hardening developed in the lower strength web on the moment capacity was reported.

Table 1: Summary of hybrid I-section bending tests.

Reference	Loading scenario	Web-to-flange yield strength ratio f_{yw}/f_{yf}	Web slenderness λ_w	Number of specimens
[1]	4PB	0.33, 0.5	2.9~3.5	2
[2]	4PB	0.36	8.8~18.6	5
[4,5]	4PB	0.72	3.7~9.1	4
	3PB		3.7~9.1	2
[10]	3PB	0.53	2.3~3.8	3
[11]	4PB	0.77	2.1~3.9	3
[12]	4PB	0.48, 0.69, 0.82	1.6~2.4	5
	3PB	0.69, 0.71, 0.82	1.4~2.1	7
[13]	3PB	0.51	0.7~1.6	10
[14]	3PB	0.51	0.9	2

American and European standards for the design of steel bridges [6,7,8] that were released in the early 2000s have stipulated specific provisions for the hybrid design of I-sections under flexure. The AASHTO specification [6] requires that the web yield strength f_{yw} be no less than 70 percent of the flange yield strength f_{yf} and 250 MPa, while Eurocode 3 [7,8] allows for hybrid girders with f_{yf}/f_{yw} ratios up to 2. Both codes specify that the flange yield strength should be used for the determination of web class in hybrid sections. Therefore, the web slenderness expressed by Equation (1) is based on f_{yf}. It is worth noting that AASHTO [6] also provides simplified calculation methods for the redistribution moment of I-sections in negative bending. These methods are based on three-point bending results [9], but are only permitted for hybrid girders with f_{yf} not exceeding 485 MPa and $f_{yw}/f_{yf} \geq 0.7$.

The moment-inelastic rotation curves specified for moment redistribution at the interior pier in this code were evaluated by Ito et al. [10]. It has been demonstrated to provide safe predictions for hybrid sections with $f_{yw}/f_{yf} = 0.53$. Several experimental investigations have also been conducted in the last decade [10-14], as listed in Table 1. However, the range of web slenderness is relatively narrow, particularly for I-girders under moment gradient.

To this end, focusing on the local buckling behaviour, a comprehensive experimental study on hybrid I-sections was performed through three-point and four-point bending series tests in this study. A total of eighteen I-sections made of Q690 flange plates were tested, covering a wide range of web slenderness, including three web strength grades-Q690, Q460 and Q355. The failure mode and the moment-rotation characteristics of I-girders were reported. Additionally, the cross-section classification methodologies in AASHTO specification and Eurocode 3, as well as the consideration of moment redistribution in the AASHTO specification was discussed against the test data.

2 CODIFIED DESIGN METHODS FOR HYBRID I-GIRDERS

For illustrative purposes, the codified design methods for hybrid I-girders are first presented herein. Table 2 presents the cross-section classification methodologies in the current American and European standards for the design of steel bridges [7-8,15-17]. In this table, R_{cap} is the rotation capacity at moments between the first full yielding of section ($M = M_p$) and the occasion when M drops to M_p; M_u is the ultimate (maximum) moment capacity; M_p and M_y represent the

full plastic moment and yield moment of sections under flexure, of which the stress distribution for hybrid I-sections is set out in Figure 1. It can be observed from this figure that for hybrid I-sections, when the outset flange edge yields, there is one portion of the web has fallen into the plastic stage.

Table 2: Definition of each class for cross-sections subjected to flexure in codes.

Required flexural performance	AASHTO specification			Eurocode 3		
	Cross-section class	Slenderness limit		Cross-section class	Slenderness limit	
		Flange	Web		Flange	Web
$R_{cap} \geq 3$ and $M_u \geq M_p$	Compact	0.38ε	3.76ε	Class 1	0.31ε	2.46ε
$M_u \geq M_p$, but $R_{cap} < 3$	Noncompact	[a] $0.56\sqrt{E/f_{yr}}$	[b] $\left(3.1+\frac{5.0}{\alpha_{wc}}\right)\varepsilon$	Class 2	0.34ε	2.84ε
$M_p > M_u \geq M_y$	Noncompact			Class 3	0.48ε	4.25ε
$M_y > M_u$	Slender	-		Class 4	-	

Note: For the doubly symmetric I-shaped sections, $\varepsilon = \sqrt{E / f_{yf}}$.

[a] f_{yr} is taken as the smaller of $0.7f_{yf}$ and f_{yw}, but not less than $0.5f_{yf}$.

[b] α_{wc} is ratio of two times the web area in compression to the area of the compression flange, but $4.6 \leq (3.1+5.0/\alpha_{wc}) \leq 5.7$.

(a) Full plastic moment M_p (b) Yield moment M_y

Figure 1: Stress distribution for hybrid I-section.

The codified limiting width-to-thickness ratios for compression elements in doubly symmetric I-sections with $f_{y,nom}$ up to 690 MPa are presented in Table 2. In AASHTO specification, a factor k_c is adopted to account for the flange and web local buckling interaction [17]. Therefore, as set out in Table 2, the slenderness limit differentiating noncompact and slender flanges is not a constant magnitude. This table shows an inconsistency in the limiting slenderness ratios for flange and web plate elements between American and European standards. It is worth noting that AASHTO specification [15] employed a hybrid factor R_h to consider the effect of lower web strength for hybrid sections, and Equation (2) serves as an alternative limiting slenderness differentiating compact and noncompact web.

$$\frac{h_w}{t_w} = \frac{\sqrt{E/f_{yf}}}{\left(0.54\frac{M_p}{R_h M_y} - 0.09\right)^2} \tag{2}$$

Besides, as noted in introduction, based on the research of Barth et al. [9,19], AASHTO specification simplifies the calculation of redistribution moments for interior-pier I-sections with $f_{y,nom}$ up to 485 MPa in continuous-span bridges, which does not require an inelastic analysis. One approach is based on the effective plastic moment M_{pe} determined at an estimated plastic rotation of 0.03 radians (at the strength limit state). Another is a refined method by applying direct analysis of nominal moment M_n-plastic rotation θ_{pl} curve shown by Figure 2. In

this figure, M_n denotes the nominal flexural strength of a section; θ_{pl} is the plastic rotation, θ_{RL} denotes the specified plastic rotation at which the section moment nominally begins to decrease. The ultra-compact web, exhibiting the enhanced moment-rotation characteristics, is particularly defined in the consideration of redistribution moment. The ultra-compact web limiting slenderness ratio is given by Equation (3).

$$\frac{h_w}{t_w} \le 2.3\sqrt{\frac{E}{f_{yf}}} \tag{3}$$

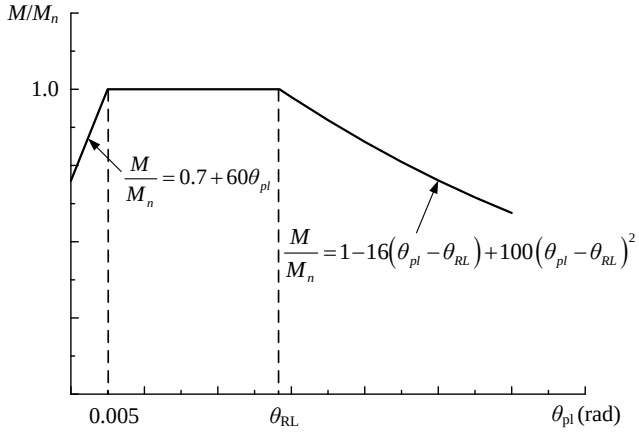

Figure 2: Nominal moment-plastic rotation curve in AASHTO specification.

3 EXPERIMENTAL STUDY

3.1 Test specimens

A total of eighteen beam tests, encompassing two loading scenarios of three-point (moment gradient) and four-point (uniform moment) bending, were carried out in this study. Three web strength grades-Q690 ($f_{y,nom}$ =690 MPa), Q460 ($f_{y,nom}$ =460 MPa) and Q355 ($f_{y,nom}$ =355 MPa) were examined for I-sections with Q690 flange plates. In other words, two groups of hybrid I-sections with f_{yw}/f_{yf} ≈0.51 and 0.67 were studied, together with their homogeneous HSS counterparts.

The flange plate elements of all the examined I-sections were designed to be compact with a thickness of 10 mm and a width of 110 mm, whilst three web width-to-thickness ratios were employed for each series (i.e., moment gradient and uniform moment test series). Table 3 tabulates the main geometrical characteristics of tested I-girders. The nomenclature of test specimens implies the loading scenario, section height and web strength grade of I-sections, e.g., "4P-H350-460W" is a four-point loaded specimen with 350 mm section height, of which the web is made of Q460 steel plate. In this table, L indicates the clear span between end supports; L_c denotes the panel length adjacent to the three-point loaded girders (350 mm in this study) or represents the length of central panel with uniform moment for four-point loaded ones-700 mm in this study, as illustrated in Figure 3.

The web classes of I-sections in accordance with American and European codes are also displayed in Table 3. In this table, for "3P-H230" specimens, "UC" in parentheses means that the web is defined as ultracompact according to Equation (3); For "4P-H440-355W", the web is noncompact according to the web limiting ratios in Table 2 but categorised as a compact one using the R_h-dependent limit-Equation (2). It can be seen from this table that I-sections with lower strength web have lower R_h values. With the non-dimensional web slenderness varying from 1.8 to 4.4, the web plates cover all the classes in Eurocode 3 (i.e., Class 1 to Class 4), and

nonslender elements are involved conforming to the American provision. Sufficient stiffeners and lateral bracings were set to exclude the influence of shear buckling and lateral torsional buckling failure modes.

Table 3: Main geometrical characteristics of I-section test specimens.

Series	Specimen	H	h_w	L	R_h	$\frac{h_w}{t_w}\sqrt{\frac{f_{yf}}{E}}$	Web class	
							AASHTO specification	Eurocode 3
3PB	3P-H230-690W	230	210	3400	1.0	2.0	C(UC)	1
	3P-H230-460W				0.96	2.1	C(UC)	1
	3P-H230-355W				0.92	1.9	C(UC)	1
	3P-H310-690W	310	290	3400	1.0	2.8	C	2
	3P-H310-460W				0.96	2.9	C	3
	3P-H310-355W				0.92	2.7	C	2
	3P-H350-690W	350	330	3900	1.0	3.1	C	3
	3P-H350-460W				0.95	3.3	C	3
	3P-H350-355W				0.91	3.0	C	3
4PB	4P-H310-690W	310	290	3300	1.0	2.9	C	2
	4P-H310-460W				0.96	3.0	C	3
	4P-H310-355W				0.92	2.7	C	2
	4P-H350-690W	350	330	3300	1.0	3.2	C	3
	4P-H350-460W				0.96	3.4	C	3
	4P-H350-355W				0.92	3.1	C	3
	4P-H440-690W	440	420	3300	1.0	4.2	N	3
	4P-H440-460W				0.95	4.2	N	4
	4P-H440-355W				0.91	4.3	N (C)	4

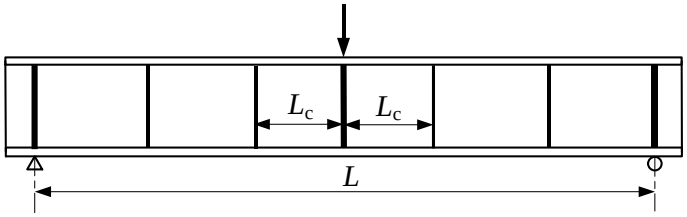

(a) Three-point bending

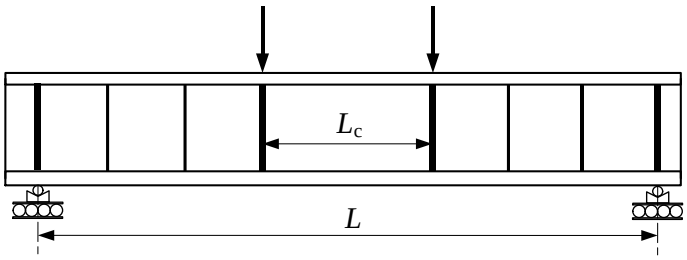

(b) Four-point bending

Figure 3: Test configuration of I-section test specimens.

3.2 Test results

Figure 4 shows the representative failure mode of tested I-girders, where the antisymmetric local deformation of flange and web plates was observed at the midspan of test specimens. For three-point loaded I-sections, the plates adjacent to central load point deformed locally (Figure 4(a)); for I-sections subjected to uniform bending, the local buckling of thin plates can be discovered in the center (Figure 4(b)).

(a) Three-point bending

(b) Four-point bending

Figure 4: Representative failure mode of test specimens.

The moment-rotation characteristics value of test specimens is given in Table 4. For the three-point loaded I-section beam specimens, the rotation at which M drops to 95%M_p (denoted as $R_{cap,95}$ in Table 4) is taken as a criterion for member ductility, since the centralised stress distribution zone has an adverse on the rotation capacity [19]. Due to the contact between loading block and lateral restraint, tests of "3P-H230-460W", "3P-H230-355W" and "3P-H310-355W" specimens were stopped prior to M dropping to M_p, the rotation capacity of these I-sections given in Table 4 cannot reflect their actual ductility. Seen from this table, all the I-girders are able to achieve the full plastic moment M_p with a value of $M_{u,test}/M_p$ greater than 1.0, and the I-section with lower strength web is found to exhibit greater rotation capacity.

Table 4: Moment-rotation characteristics of I-section test specimens.

Series	Specimen	$M_{u,test}$ (kN·m)	M_p (kN·m)	$M_{u,test}/M_p$	R_{cap} ($R_{cap,95}$)	$M_{n,AASHTO}/M_{u,test}$	$M_{n,EC3}/M_{u,test}$
3PB[a]	3P-H230-690W	270.9	244.4	1.11	2.17	0.90	0.90
	3P-H230-460W	248.3	226.2	1.10	>2.41[b]	0.91	0.91
	3P-H230-355W	248.6	218.6	1.14	>2.97[b]	0.88	0.88
	3P-H310-690W	393.3	361.7	1.09	2.35	0.92	0.92
	3P-H310-460W	343.5	326.1	1.05	1.74	0.95	0.89
	3P-H310-355W	347.5	307.5	1.13	>2.56[b]	0.88	0.88
	3P-H350-690W	456.4	429.1	1.06	0.80	0.94	0.82
	3P-H350-460W	405.6	379.5	1.07	0.95	0.93	0.87
	3P-H350-355W	397.9	361.0	1.10	1.66	0.91	0.86
4PB	4P-H310-690W	386.1	356.4	1.08	1.43	0.93	0.93
	4P-H310-460W	343.3	327.0	1.05	1.47	0.95	0.89
	4P-H310-355W	333.6	311.7	1.07	2.01	0.93	0.93
	4P-H350-690W	449.0	428.0	1.05	0.91	0.95	0.83
	4P-H350-460W	400.5	373.8	1.07	1.54	0.93	0.88
	4P-H350-355W	397.3	363.8	1.07	2.38	0.93	0.89
	4P-H440-690W	583.3	582.6	1.00	0.32	0.97	0.86
	4P-H440-460W	524.6	508.0	1.03	0.72	0.97	0.93
	4P-H440-355W	507.0	482.4	1.05	0.98	0.95	0.92
Mean						0.93	0.89
Coefficient of Variation						0.028	0.035

Note: [a] $R_{cap,95}$ is considered for I-sections subjected to three-point bending; [b] test was stopped prior to M dropping to the desired moment capacity.

The normalised moment-rotation curves of I-sections with a section height of 440 mm are shown in Figure 5 as a representative. It is apparent from this figure that the I-section with a lower strength web not only presents better ductility, but also exhibits greater values of $M_{u,test}/M_p$. This finding is in line with their R_h-dependent web classes according to AASHTO specification presented in Table 3.

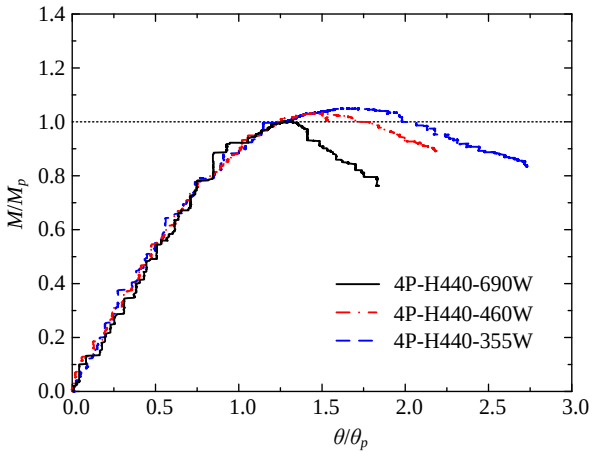

Figure 5: Normalised moment-rotation curves of "4P-H440" specimens.

In addition, test results of I-sections with 350 mm section height under three-point and four-point bending are compared in Figure 6. It can be observed that I-sections under moment gradient possess the greater normalised moment resistance $M_{u,test}/M_p$ than the uniform moment counterparts, whereas pure bending I-sections experiences preferable rotation capacity. This observation supports the theoretical viewpoints that the yielding of a four-point loaded beam will spread over the uniform moment segment, whilst the yielding of a three-point loaded beam is confined to the region adjacent to the loading point and cannot spread unless moment is increased [20].

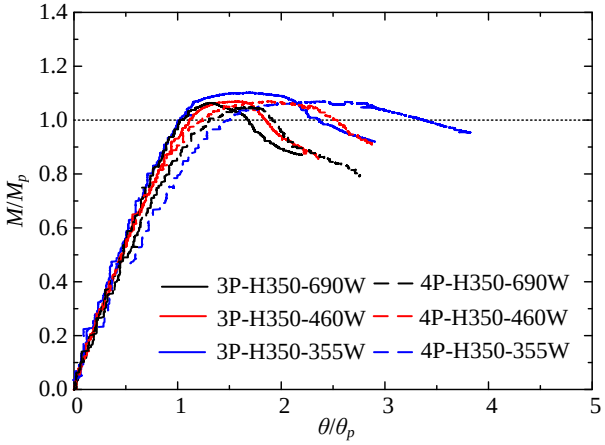

Figure 6: Comparison of normalised moment-rotation curves between three-point and four-point bending I-sections.

4 DISCUSSION OF CURRENT DESIGN PROVISIONS

4.1 General

Design provisions on the hybrid design in the current American and European specifications for the design of steel bridges [7-8, 15-17] were assessed against the test results in the following

subsections, including the codified cross-section classification methodologies, moment capacity design formulas, as well as the redistribution moment calculation methods for the interior pier of continuous span bridges.

4.2 Cross-section classification and moment capacity

Figure 7 compares the test data and the cross-section classification methodologies in European code and AASHTO specification. In this figure, the noncompact limiting ratio is conservatively selected to be 5.28, which is determined based on the geometry of the I-section with the slenderest web- "4P-H440" specimens. The prematurely stopped specimens are highlighted in this figure by a star-shaped symbol. All the data points of $M_{u,test}/M_p$ are shown to be above the reference line of unity in Figure 7, revealing that all the I-sections are able to meet the codified demand in moment resistance. However, as illustrated in Figure 7(a), most data points of compact web I-sections fall below the reference line of R_{cap} ($R_{cap,95}$) =3, indicating that I-girders with the web plate designed as compact conforming to AASHTO specification fail to meet the ductility requirement; Meanwhile, among Class 1 "3P-H230" specimens, only the I-section made of Q355 web is demonstrated to achieve the rotation capacity of 3, as shown in Figure 7(b).

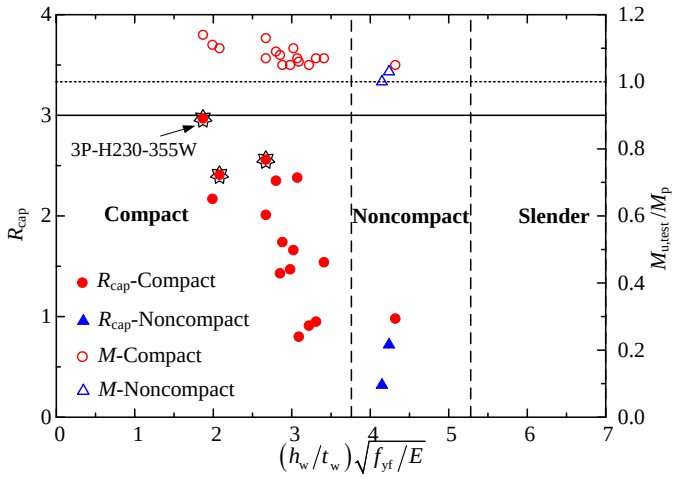

(a) AASHTO specification

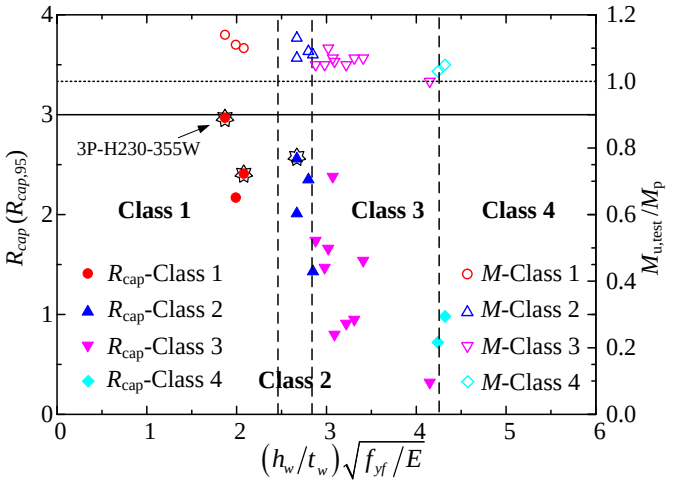

(b) Eurocode 3

Figure 7: Comparison of test data and the cross-section classification in codes.

The predicted-to-test flexural strength ratios in accordance with AASHTO specification ($M_{n,AASHTO}/M_{u,test}$) and Eurocode 3 ($M_{n,EC3}/M_{u,test}$) are tabulated in Table 6. In AASHTO

specification [15], two sets of moment capacity design expressions are provided for I-sections under flexure (i.e., Section 6.10.8 and Appendix A6). To be specific, Section 6.10.8 is stipulated for all the non-composite I-sections, limiting the nominal flexural strength $M_{n,AASHTO}$ to the moment at which compression flange initially yields. Appendix A6 offers an optional calculation method for I-sections with compact or noncompact web, so that the full plastic moment M_p of these I-sections has a chance to be fully mobilised. As presented in Table 4, the web plate of all I-girders is non-slender (i.e., compact and noncompact), the provisions in Appendix 6 were thus assessed in this study. The compared statistical analysis results- mean and Coefficient of Variation in Table 6 reveals that AASHTO specification generally yields closer cross-sectional resistance predictions to the test data in comparison to those derived from Eurocode 3.

4.3 Redistribution moment at the interior pier

The redistribution moment calculation methods prescribed in AASHTO specification [15] are discussed against the moment-rotation characteristics of three-point loaded I-sections. The moment-plastic rotation curves of "3PB" specimens are set out in Figure 8, together with the nominal curve stipulated by AASHTO (notated as AASHTO curve). The plastic rotation θ_{pl} in this figure is calculated by subtracting the theoretical elastic rotation from the total end rotation of girders [18,20]. It can be seen from this figure that the linear pre-peak zone of AASHTO curve (from $0.7M_n$ rising to M_n) can roughly capture the flexural behaviour of both HSS and hybrid I-girders prior to reaching the ultimate moment resistance, whilst the plateau and descending portions of AASHTO curve are observed to be over-conservative for the investigated I-sections.

The effective plastic moment-to-nominal design moment resistance ratio M_{pe}/M_n for each section dimension is also described in Figure 8, with the highlighted plastic rotation of 0.03 and 0.063 radians. The value of 0.03 radian, stated by AASHTO [15] to determine M_{pe}, is the upper bound for the recommended inelastic rotation at pier sections [22]; 0.063 radian is the plastic rotation required for buildings and bridges suggested by Haaijer et al. [23]. As shown in Table 4, among "3PB" test series, I-sections with 230 mm section height are featured with ultracompact web, M_{pe} is thus equivalent to M_n in Figure 8(a); for the remaining I-sections with compact web, the value of M_{pe}/M_n is less than unity. What stands out in this figure is that the normalised flexural strength M/M_n of I-girders at both 0.03 and 0.063 radians is greater than the specified M_{pe}/M_n, indicating that the expressions of M_{pe} in AASHTO specification is safe for HSS and hybrid I-girders investigated in this study, despite the steel strengths and web-to-flange ratios of these sections are out of the scope of designed rules: $f_{yf} \leq 485$ MPa and $f_{yw}/f_{yf} \geq 0.7$.

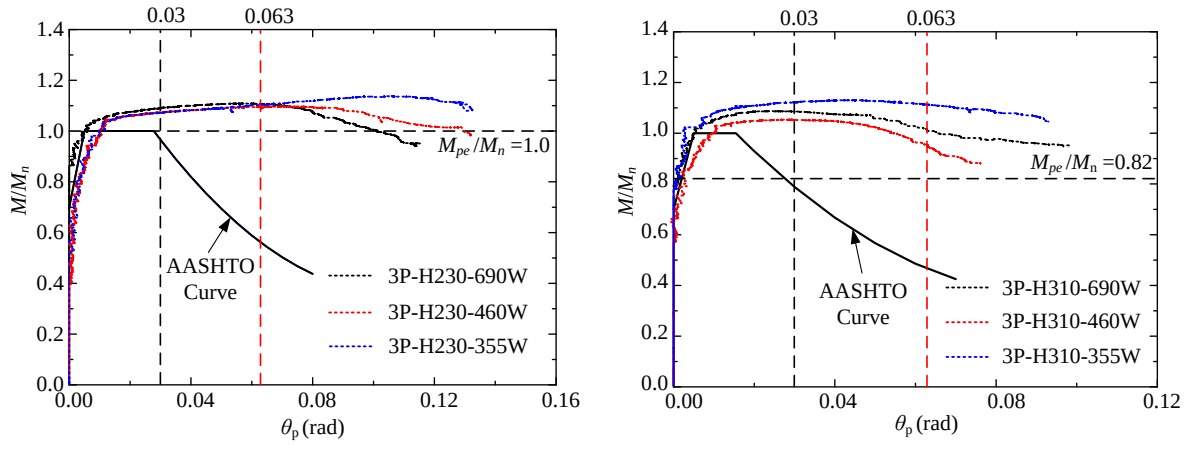

(a) "3P-H230" specimens

(b) "3P-H310" specimens

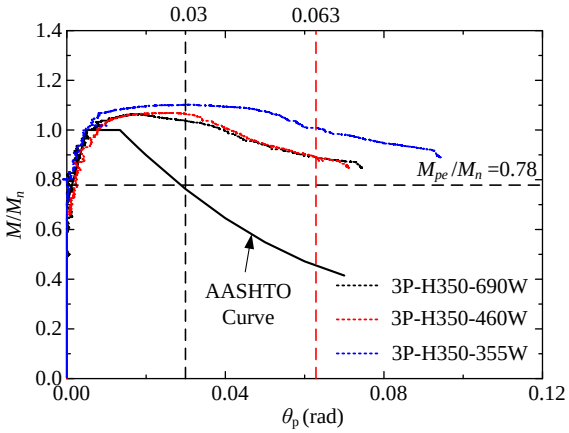

(c) "3P-H350" specimens

Figure 8: Comparison of test data and the consideration of redistribution moment in AASHTO specification.

5 CONCLUSIONS

In this study, a test program incorporating three-point and four-point bending was carried out to investigate the local buckling behaviour of hybrid I-sections. A total of eighteen I-girders with Q690 flanges with varied web strength grades and web slendernesses were examined. Two groups of hybrid I-sections featured with Q460 and Q355 webs were studied, along with homogenous HSS Q690 counterparts. The results of the moment-rotation characteristics of test specimens showed that hybrid I-sections with lower strength web presents preferable rotation capacity.

The cross-section classification methodologies and design resistance provisions regulated in AASHTO specification and Eurocode 3, as well as the consideration of redistribution moment stipulated by AASHTO were evaluated against the test data. The comparison of experimental results and design moment resistance showed that I-sections with compact web conforming to AASHTO specification fail to meet the ductility requirement, and among Class 1 sections in accordance with Eurocode 3, only the I-sections made of Q355 web can achieve the required rotation capacity. However, in terms of moment resistance compared with Eurocode 3, the design expressions in AASHTO specification provide closer results to the test data in this study. Moreover, the redistribution moment calculation methods in AASHTO specification are found to be safe enough to be applicable to hybrid I-sections fabricated from Q690 flanges with the ratio of web to flange yield strength about 0.5, which is not within the scope of this standard.

Further modelling work will be performed for a comprehensive investigation and assessment of the local buckling behaviour of hybrid I-sections.

REFERENCES

[1] Lew H.S. and Toprac A.A., "*Static tests on hybrid plate girders*", Austin: Center for Highway Research, TX: The University of Texas, 1967.

[2] Frost R.W. and Schilling C.G., "Behavior of hybrid beams subjected to static loads", *Journal of the Structural Division*, **90**(3), 55-88, 1964.

[3] Joint American Society of Civil Engineers-AASHO Committee on Flexural Members, "Design of hybrid steel beams", *Journal of the Structural Division*, **94**(6), 1397-1426, 1968.

[4] Kamtekar A.G., Dwight J.B. and Threlfall B.D., "*Tests on hybrid plate girders (Report 2)*", Report No. CUED/C-Struct/TR Cambridge, 1972.

[5] Kamtekar A.G., Dwight J.B. and Threlfall B.D., "*Tests on hybrid plate girders (Report 3)*", Report No. CUED/C-Struct/TR41 Cambridge, 1974.

[6] American Association of State Highway and Transportation Officials (AASHTO), *AASHTO LRFD bridge Design Specification, 4th Ed*, Washington, DC: AASHTO, 2007.

[7] European Committee for Standardization (CEN), *Design of steel structures, part 1.5: Plated structural elements, EN 1993-1-5, Eurocode 3*, Brussels, Belgium: CEN, 2006.

[8] European Committee for Standardization (CEN), *Design of steel structures, part 2: Design of steel structures, Eurocode 3*, Brussels, Belgium: CEN, 2006.

[9] Barth K. E., Hartnagel B. A., White D. W. and Barker M.G., "Recommended procedures for simplified inelastic design of steel I-girder bridges", *Journal of Bridge Engineering*, **9**(3), 230-242, 2004.

[10] Ito M., Nozaka K., Shirosaki T. and Yamasaki K., "Experimental study on moment–plastic rotation capacity of hybrid beams", *Journal of Bridge Engineering*, **10**(4), 490-496, 2005.

[11] Shokouhian M. and Shi Y.J., "Flexural strength of hybrid steel I-beams based on slenderness", *Engineering Structures*, **93**, 114-128, 2015.

[12] Wang C.S., Duan L. Chen Y.F. and Wang S.C., "Flexural behavior and ductility of hybrid high performance steel I-girders", *Journal of Constructional Steel Research*, **125**, 1-14, 2016.

[13] Bartsch H., Eyben F., Pauli G., Schaffrath S. and Feldmann M., "Experimental and numerical investigations on the rotation capacity of high-strength steel beams", *Journal of Structural Engineering*, **147**(6), 04021067, 2021.

[14] Zhu Y.F., Yun X. and Gardner L., "Behaviour and design of high strength steel homogeneous and hybrid welded I-section beams", *Engineering Structures*, **275**, 115275, 2023.

[15] American Association of State Highway and Transportation Officials (AASHTO), *AASHTO LRFD Bridge Design Specification, 9th Ed*, Washington, DC: AASHTO, 2020.

[16] European Committee for Standardization (CEN), *Design of steel structures, part 1.1: General rules and rules for buildings, Eurocode 3, EN 1993-1-1*, Brussels, Belgium: CEN, 2005

[17] European Committee for Standardization (CEN), *Design of steel structures, part 1.12: Additional rules for the extension of EN 1993 up to steel grades S700, EN 1993-1-12*, Eurocode 3, Brussels, Belgium: CEN, 2007.

[18] Johnson D.L., "An investigation into the interaction of flanges and webs in wide-flange shapes", *Proceedings of the Annual Technical Session and Meeting*, Cleveland, OH, April 16-17, 1985, SSRC, Bethlehem, PA, pp. 397–405, 1985.

[19] White D. W., Ramirez J. A. and Barth K. E., "*Moment-Rotation Relationship for Unified Auto-Stress Design of Continuous-Span Bridge Beam and Girders*", Publication FHWA/IN/JTRP-97/08，Joint Transportation Research Program, Indiana Department of Transportation and Purdue University, West Lafayette, Indiana, 1997.

[20] Galambos T.V., "*Deformation and energy absorption capacity of steel structures in the inelastic range*", Bulletin No. 8. New York, American Iron and Steel Institute, 1968.

[21] Barth K.E., "*Moment-rotation characteristics for inelastic design of steel bridge beam and girders*", Purdue University, 1996.

[22] Schilling C. G., Barker M.G., Dishongh B.E., and Hartnagel B.A., "*Inelastic design procedures and specifications*", Final report submitted to the American Iron and steel Institute, Washington, DC, 1997.

[23] Haaijer G., "Economy of high strength steel structural members", *Transactions of the American Society of Civil Engineers*, **128**(2), 820-842, 1963.